

Direct Transition to Spatiotem poral Chaos in Low Prandtl Number Fluids

Hao-wen Xie¹, Xiao-jin Li² and J.D. Gunton²¹ Department of Physics and Astronomy, Bowling Green State University, Bowling Green, OH 43403.² Department of Physics, Lehigh University, 16 Memorial Drive East, Bethlehem, PA 18015.

(March 9, 2019)

We present the first large scale numerical simulation of three-dimensional Rayleigh-Bénard convection near onset, under free-free boundary conditions for a fluid of Prandtl number $\text{Pr} = 0.5$. We find that a spatiotem porally chaotic state emerges immediately above onset, which we investigate as a function of the reduced control parameter $\text{R} = (R - R_c)/R_c$. We conclude that the transition from conduction to spatiotem poral chaos is second order and of "mean field" character. We also present a simple theory for the time-averaged convective current. Finally, we show that the time-averaged structure factor satisfies a scaling behavior with respect to the correlation length near onset.

PACS numbers: 47.20.Bp, 47.54.+r, 47.20.Lz, 47.27.Te

One of the most fascinating examples of self-organized phenomena in nature is the symmetry breaking, pattern formation in non-equilibrium systems [1]. A paradigm of such pattern formation is Rayleigh-Bénard convection [2], which occurs when a thin horizontal fluid layer is heated from below. In general, the dynamics of Rayleigh-Bénard convection depends on the Rayleigh number R , the Prandtl number of the fluid and the aspect ratio of the system. Busse and his collaborators [3] have studied extensively the stability domain, known as the "Busse Balloon", of parallel rolls as a function of wavenumber k and Rayleigh number R , for various Prandtl numbers. It is well known that in a laterally infinite system with rigid-rigid boundaries, there exists a stable, time independent parallel roll state near the onset of convection for all R . However, in the case of free-free boundaries at sufficiently low Prandtl numbers ($\text{Pr} < 0.543$), Siggia and Zippelius [4] [5] and Busse and Bolton [6] found surprisingly that parallel rolls are unstable with respect to the skewed-varicose instability immediately above onset. An interesting implication of their results is: Because none of the modes (whose horizontal wave-vector $\mathbf{k} \parallel \mathbf{k}_c$, the onset wavenumber) is chosen as an orientation for steady rolls, the convective patterns near onset might be random in two-dimensional horizontal space and in time. If so, then the transition to spatiotem poral chaos (STC) occurs right at the critical Rayleigh number R_c , where the bifurcation from conduction to convection usually takes place. It is thus possible that this provides another example of a direct transition from conduction to STC, in addition to the Kuppers-Lortz transition [7].

In this paper, we present the results of the first large scale numerical simulation of the three dimensional hydrodynamic equations, using the Boussinesq approximation, for a low Prandtl number fluid ($\text{Pr} = 0.5$) with free-free boundary conditions. We find that the convective state just above onset is spatiotem porally chaotic, which is evident from the snapshot images of the vertical velocity field and from the dynamical behavior of three important global quantities: the viscous dissipation energy, the thermal dissipation energy and the work done by the

buoyancy force. Our method suggests that by studying the dynamical behavior of some global quantities of systems which exhibit STC, one may obtain valuable information about the temporal chaos of these systems. We also measure the fractal dimensions of these global quantities and find a value of about 1.4. In addition, we investigate the nature of the conduction to STC transition, as well as certain properties of the spatiotem porally chaotic state. Our results for the correlation length suggest that the transition is second order, with a mean field power law behavior. In comparison recent experimental results for the Kuppers-Lortz transition are not consistent with a mean field power law behavior [8]. Thus this low Prandtl number, free-free boundary condition system seems to provide the simplest example of a transition to STC for which one might be able to develop a theory. Indeed, we present below a simple but rather accurate theory for the behavior of the time-averaged convective current as a function of the reduced control parameter,

$\text{R} = (R - R_c)/R_c$. Finally, we show that the time-averaged structure factor (power spectrum) exhibits a scaling behavior with respect to the correlation length similar to that found in critical phenomena.

The Boussinesq equations, which describe the evolution of the velocity field $\mathbf{u}(x, y, z, t) = (u, v, w)$ and the deviation of the temperature field $\theta(x, y, z, t)$ from the conductive profile, can be written in dimensionless form as

$$\begin{aligned} & \nabla \cdot \mathbf{u} = 0; \\ & \partial \mathbf{u} / \partial t + (\mathbf{u} \cdot \nabla) \mathbf{u} = -\nabla p + \mathbf{e}_z + \text{Pr}^2 \mathbf{u}; \\ & \partial \theta / \partial t + \mathbf{u} \cdot \nabla \theta = \mathbf{f} + \text{Pr} \mathbf{R}; \end{aligned} \quad (1)$$

where \mathbf{e}_z is the unit vector in the vertical z -direction. The dimensionless control parameters for the problem are the Rayleigh number R and the Prandtl number Pr . The efficient Marker-and-Cell (MAC) [9] [10] numerical technique is employed. The boundary conditions for the velocities are free-slip at the upper and lower surfaces, and no-slip at the sidewalls. The temperature deviation

is zero on the top and bottom surfaces, while the temperature gradient $\nabla \theta$ normal to the sidewall is set to

zero. In the idealized limit of a laterally infinite system, the critical Rayleigh number $R_c = 27^4 = 4$ and the onset wavenumber $k_c = \sqrt{2}$. Our parameters are $\beta = 0.5$ and $0.03 < \beta < 0.5$, where $\beta = (R - R_c)/R_c$ is the reduced Rayleigh number. We use mesh points $N_x = N_y = N_z = 256 \times 256 \times 18$ and a grid size $x = y = 60/256$, $z = 1/18$ for an aspect ratio (size/thickness) $= 60$ in the simulation.

For the low Prandtl number studied here, the convective pattern near onset has an irregular space-time dependence. In Figure 1 we show a snapshot in space of the vertical velocity field $w(x, y, z = 1/2)$ from the numerical simulation at $\beta = 0.1$. In this image, the apparently disorganized spatial pattern consists of superimposed rolls with many different orientations. The time evolution of these rolls is through an interface motion, which maintains the type of spatial disorder shown in Figure 1. Similar images are found for other values of β . It is obvious from such images that the convection pattern near onset is random in space.

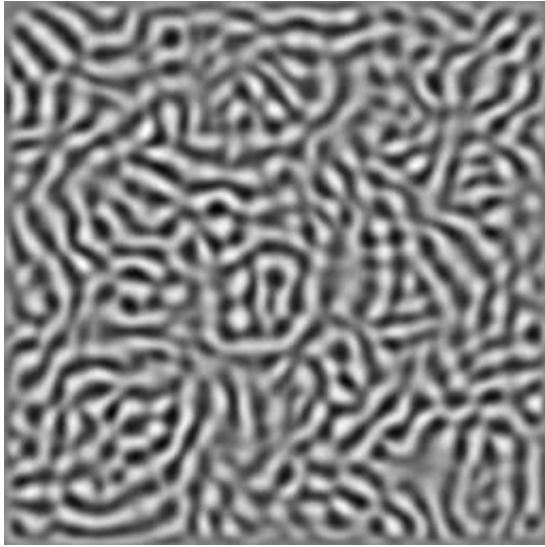


FIG. 1. A typical snapshot of the spatially disorganized pattern in the cell. Dark regions correspond to hot rising fluid and white regions correspond to cold descending fluid. The vertical velocity field $w(x, y, z = 1/2)$ for $\beta = 0.1$ is shown here.

To illustrate the temporal chaos of the system, we now investigate the dynamics of the global quantities which characterize the underlying physics of Rayleigh-Bénard convection. Using $\langle f \rangle$ to denote the average of f over the whole system and taking into account the boundary conditions as well as the incompressibility condition, we obtain $\frac{1}{2} \frac{d}{dt} \langle u_i \rangle = \langle F_1(t) \rangle - \langle F_2(t) \rangle$, and $\frac{1}{2} \frac{d}{dt} \langle h^2 \rangle = \langle F_4(t) \rangle - \langle F_3(t) \rangle$, where (a) $F_1 = \frac{1}{2} \int h(\partial u_i / \partial x_j + \partial u_j / \partial x_i)^2 d\Omega$ is the kinetic energy dissipated by the viscosity; (b) $F_2 = \int h w d\Omega$ is the work done by the buoyancy force; (c) $F_3 = \int h r d\Omega$ is the dissipative thermal energy (generation of entropy) due to temperature fluctuations; and (d) $F_4 = \int R h w d\Omega = (R F_2) / \beta$ is the flow of the entropy

fluctuations carried by the vertical velocity. It is clear that in the special case of steady state ($\frac{d}{dt} = 0$), one recovers the condition $F_1 = F_2$ and $F_4 = F_3$. These global quantities provide us with a complete description of "energy balance" in the Rayleigh-Bénard system.

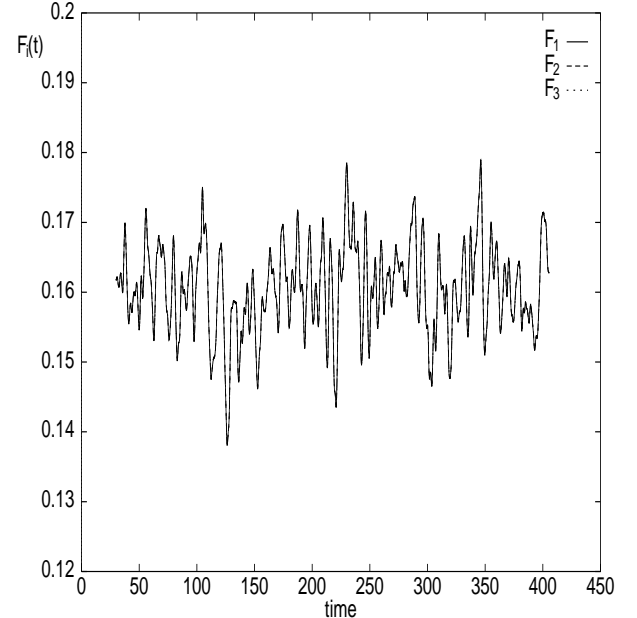


FIG. 2. A plot of global quantities $F_1(t)$, $F_2(t)$ and $F_3(t)$ as functions of time for $\beta = 0.2$. Note that they lie on top of each other; time is in units of vertical thermal diffusion time $t_v = d^2/\kappa = 1$.

We plot a representative time series of these quantities, $F_1(t)$, $F_2(t)$ and $F_3(t)$, in Figure 2 for $\beta = 0.2$. We have rescaled F_1 , F_2 by R_c , and F_3 by $R R_c$ so that we have $F_1 = F_2 = F_3$ in a steady state. (Note that F_4 is simply related to F_2 by the factor R/β .) The most important implication of this figure is the apparent chaotic behavior of these quantities over the time interval that is accessible to us. To be more concrete, we apply the Grassberger and Procaccia method [11] to compute the fractal dimensions D_f for these quantities and find $D_f = 1.42 \pm 0.02$. This of course is different from the fractal dimension that is normally used to characterize STC, which diverges with the system size. As noted earlier, we believe that such global quantities might provide a relatively simple way to characterize the temporally chaotic nature of spatiotemporally chaotic states such as studied here, although data over a longer time interval will be necessary for such an analysis. It is also interesting to observe that the dynamics of these three quantities are almost exactly the same, i.e. $F_1(t) = F_2(t) = F_3(t)$, as shown in Figure 2. In fact, this is the case for all β studied in the range $0.03 < \beta < 0.5$. This is certainly a surprising result considering the irregular spatiotemporal state we observed. However, a theoretical understanding of this can be obtained, based on the Swift-Hohenberg model and the fact that only those modes whose wavenumber is in the range k_c are excited. This result also implies that the quantity

$\zeta = F_3 = (2F_2 - F_1)$, which is often used as a variational formulation to determine the critical Rayleigh number, behaves as if the system is in a steady state.

In order to gain more insight into the nature of the transition to STC near onset, we have studied the two-dimensional structure factor (Fourier power spectrum). Since the snapshot images of the patterns appear to be isotropic azimuthally, we calculate the azimuthally averaged structure factor, and then average the images over time, to obtain the time-averaged structure factor $S(k)$. The function $kS(k)$ is shown for several different values of ϵ in the inset in Figure 3. We also show in this figure that $kS(k)$ satisfies a scaling behavior somewhat similar to that found in critical phenomena, namely, $kS(k) = F[(k/k_{\max})^\beta]$, where β is the correlation length (defined below) and where we have normalized the integral of $S(k)$ over k -space to be unity. Here k_{\max} is the wavenumber which maximizes $kS(k)$, which we choose to give the best fit to scaling. Another interesting feature of the structure factor is associated with the power-law behavior of $S(k) \propto k^{-3}$ for large wavenumber. This feature is observed over the range of ϵ studied here. It is interesting to note that this is the same power-law behavior observed in phase separating systems, in two dimensions, where it is known as Porod's law. In both cases it results from the linear behavior of the real space correlation function, $C(r)$, for small r , where this correlation function is the azimuthal average of the inverse Fourier transform of the structure factor.

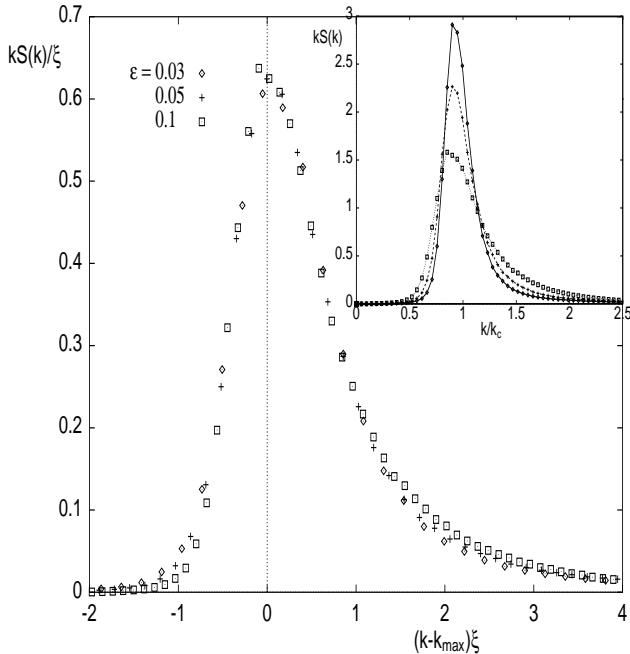


FIG. 3. A plot of $kS(k)/\zeta$ vs $x = (k/k_{\max})^\beta$, showing scaling and the scaling function $F(x)$ defined in the text. Inset: The time-averaged function $kS(k)$ vs. $k=k_c$ for $\epsilon = 0.03, 0.05$ and 0.1 .

We have also calculated the correlation length as a

function of the control parameter ϵ , where we define the correlation length through the variance of the wavenumber, i.e., $\langle k^2 \rangle = \langle k^2 \rangle_R^{1/2}$. The moment k^n is defined as $\langle k^n \rangle = \int k^n S(k) d^2k = \langle S(k) d^2k \rangle$ and $S(k)$ is the time-averaged structure factor. We find that the correlation length appears to diverge as ϵ approaches the transition point, with a power-law behavior of $\zeta = \zeta_0(\epsilon - \epsilon_c)$ with $\zeta_0 = 0.472, \epsilon_0 = 0.016, \zeta_0 = 0.82, \epsilon_0 = 0.04$ and $\zeta_c = 0.005$. (The fact that ζ_c is finite instead of zero is due to finite size effects.) The behavior of the correlation length is also consistent with a mean field power law exponent of $\beta = 0.5$ and $\zeta_0 = 0.78$. This is illustrated in Figure 4. The amplitude value ζ_0 is a factor of $2/3$ smaller than the value $\zeta_0 = k_c^{-8/3} = 1.15$ calculated from the curvature of the marginal stability curve.

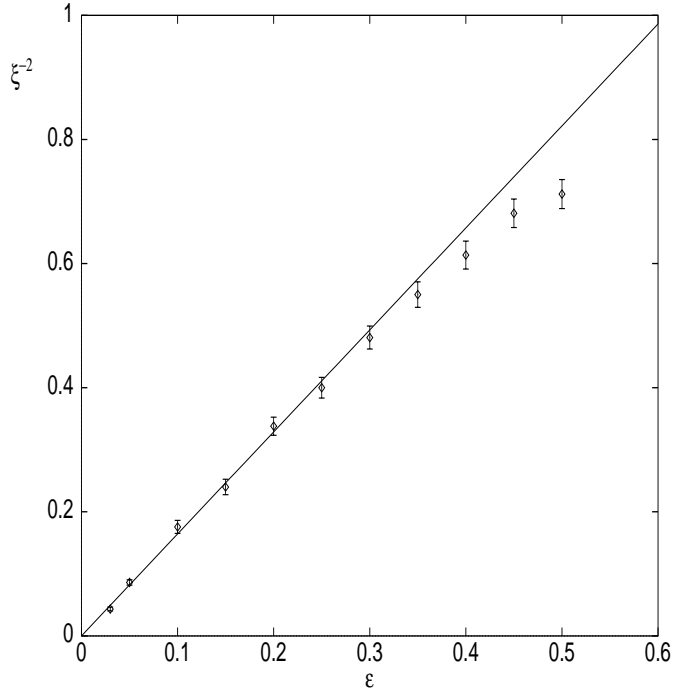


FIG. 4. A plot of ζ^2 vs. ϵ . The vertical bars indicate the standard deviation, and the solid line corresponds to $\zeta^2 = \zeta_0^2$ with $\zeta_0 = 0.78$. These data can also be fitted with a nonconventional exponent: see the text for more detail.

In order to investigate the heat transport in STC near onset, we calculate the Nusselt number $N(t) = 1 + \text{heat}$ $i=R$, which describes the ratio between the heat transport with and without convection, as a function of ϵ . The quantity $N-1$ can be fitted with a power law behavior of the form $N-1 = (\epsilon - \epsilon_c)^{-\bar{g}}$ with $\bar{g} = 1.034, \epsilon_c = 0.025, \zeta_c = 0.012$ and $\bar{g} = 1.27, \epsilon_c = 0.03$. Figure 5 shows that the time-averaged $N-1$ is also consistent with a linear relation $(\epsilon - \epsilon_c) = \bar{g}$, where $\epsilon_c = 0.01$ and $\bar{g} = 1.23$. (Again, owing to finite size effects, the value of ζ_c is nonzero.) This latter result can be understood quantitatively by considering the following simplified analysis using the

amplitude equation approach [12]. We assume that all the modes near the critical wavenumber are degenerate and equally excited. We thus limit the wave-vectors \hat{k} to the vicinity of the critical wavenumber k_c , and obtain

$$\bar{g} = \frac{P}{k_1} [2g(\hat{k} \cdot \hat{k}_1) + g(-1)g(\hat{k} \cdot \hat{k}_1)(2 \frac{\hat{k} \cdot \hat{k}_1}{k_1; \hat{k}_1, \hat{k}})]^M. \quad (1)$$

Here \hat{k} is an arbitrary reference vector, and M is the total number of modes in two dimensional Fourier space at the ring structure $\hat{k}_1 \approx k_c$. For example, for a parallel roll pattern we have $M = 2$, and $\bar{g} = [g(+1) + 2g(-1)]/2$ [12]. For the case of highly degenerate wavenumbers near k_c , the constant \bar{g} is found by taking the limit $M \rightarrow 1$. We thus obtain

$$\begin{aligned} \bar{g} &= g(-1) + (2 =) \int_0^{\pi} g(\cos \theta) d\theta \\ &= 0.855951 + 0.0458145 \theta^1 + 0.0709325 \theta^2. \end{aligned} \quad (2)$$

We have used the explicit form of $g(\cos \theta)$ given by Schlüter et al [13] for free-free boundary conditions [12]. For $\epsilon = 0.5$, we find $\bar{g} = 1.2313$, which is in surprisingly good agreement with the numerical results. We should point out that the above calculation is oversimplified and further work is in progress. We have also determined the time-averaged vertical "vortex energy" $\langle \omega_z^2 \rangle = h! \langle \omega_z^2 \rangle$, where ω_z is the vertical vorticity, as a function of ϵ from our simulations and observed a power-law behavior of $\langle \omega_z^2 \rangle \propto \epsilon^{5/2}$. The theory of this behavior is more complicated than the above and will be presented elsewhere.

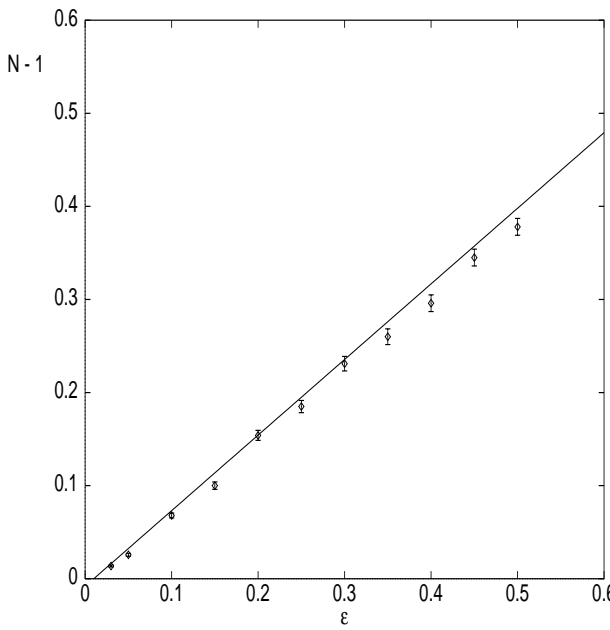


FIG. 5. Time-averaged $N-1$ vs ϵ near onset. The vertical bars indicate the standard deviation, and the solid line is the fit of $\langle \omega_z^2 \rangle = \bar{g}$ to the data with $\epsilon_c = 0.01$ and $\bar{g} = 1.23$. A slightly different fitting form is given in the text.

In summary, we have presented the first large scale numerical simulation of pattern formation in three dimensional Rayleigh-Bénard convection. We have calculated the spatial correlation length and the Nusselt number as a function of the reduced control parameter, as well as the dynamics of the viscous energy, the dissipative thermal energy and the work done by the buoyancy force which characterize the global behavior of the system. Our numerical studies suggest that the transition from the conduction state to spatiotemporal chaotic state near onset is a continuous (second order) transition, with mean field exponents for the correlation length and the time-averaged convective current. We have also illustrated that the time-averaged structure factor satisfies a scaling behavior with respect to the correlation length. We believe that more studies of scaling in STC by systematic experiments for smaller, larger aspect ratio, and with both free-free and rigid-rigid boundary conditions will be challenging and valuable.

JL and JDG are grateful to the National Science Foundation for support under Grant No. DMR-9596202. The computations were performed at the Pittsburgh Supercomputing Center and the Ohio Supercomputer Center.

- [1] M. C. Cross and P. C. Hohenberg, *Rev. Mod. Phys.* **65**, 851 (1993).
- [2] G. Ahlers, Over Two Decades of Pattern Formation, a Personal Perspective [preprint].
- [3] F. H. Busse, *Rep. Prog. Phys.* **41**, 1929 (1978).
- [4] A. Zippelius and E. D. Siggia, *Phys. Rev. A* **26**, 1788 (1982).
- [5] A. Zippelius and E. D. Siggia, *Phys. Fluids* **26**, 2905 (1983).
- [6] F. H. Busse and E. W. Bolton, *J. Fluid Mech.* **146**, 115 (1984).
- [7] G. Kuppers and D. Lortz, *J. Fluid Mech.* **35**, 609 (1969); G. Kuppers, *Phys. Lett. A* **32**, 7 (1970).
- [8] Y. Hu, R. E. Ecke and G. A. Ihlers, *Phys. Rev. Lett.* **74**, 5040 (1995).
- [9] F. H. Harlow and J. E. Welch, *Phys. Fluids* **8**, 2182 (1965).
- [10] B. D. Nichols, C. W. Hirt, and R. S. Hotchkiss, Los Alamos Scientific Lab. Rep. LA-8355 (1989).
- [11] P. Grassberger and I. Procaccia, *Phys. Rev. Lett.* **50**, 346 (1983).
- [12] M. C. Cross, *Phys. Fluids* **23**, 1727 (1980).
- [13] A. Schlüter, D. Lortz, and F. Busse, *J. Fluid Mech.* **23**, 129 (1965).